

## BARRED GALAXY PHOTOMETRY: COMPARING RESULTS FROM THE CANANEA SAMPLE WITH $N$ -BODY SIMULATIONS

E. Athanassoula<sup>1</sup>, D. A. Gadotti<sup>2</sup>, L. Carrasco<sup>3</sup>, A. Bosma<sup>1</sup>, R. E. de Souza<sup>4</sup>, and E. Recillas<sup>3</sup>

### RESUMEN

Presentamos los resultados de observaciones de galaxias barradas y de simulaciones de  $N$ -cuerpos

### ABSTRACT

We compare the results of the photometrical analysis of barred galaxies with those of a similar analysis from  $N$ -body simulations. The photometry is for a sample of nine barred galaxies observed in the  $J$  and  $K_s$  bands with the CANICA near infrared (NIR) camera at the 2.1-m telescope of the Observatorio Astrofísico Guillermo Haro (OAGH) in Cananea, Sonora, Mexico. The comparison includes radial ellipticity profiles and surface brightness (density for the  $N$ -body galaxies) profiles along the bar major and minor axes. We find very good agreement, arguing that the exchange of angular momentum within the galaxy plays a determinant role in the evolution of barred galaxies.

*Key Words:* galaxies: photometry — galaxies: structure — galaxies: evolution — galaxies: general

### 1. INTRODUCTION

The majority of disc galaxies are barred (e.g. de Vaucouleurs et al. 1991; Eskridge et al. 2000; Knapen, Shlosman & Peletier 2000; Marinova & Jogee 2007; Menendez-Delmestre et al. 2007) so that understanding the formation and evolution of bars and their relation to the remaining galactic components is an essential step towards understanding disc galaxy formation and evolution in general. We will here briefly describe some work to that avail, which compares results from photometric observations (Gadotti et al. 2007) to  $N$ -body simulations (Athanassoula & Misiriotis 2002).

### 2. $N$ -BODY SIMULATIONS

Barred galaxies evolve by internal redistribution of angular momentum. By measuring the frequencies of the orbits in  $N$ -body simulations, Athanassoula (2002, 2003) showed that angular momentum is

emitted by near-resonant material in the bar region and absorbed by near-resonant material in the outer disc or in the halo. The strength of the bar increases with the amount of angular exchanged. In fact, Athanassoula (2003) found a correlation between the angular momentum acquired by the halo and the bar strength.

$N$ -body simulations show that the properties of bars which grow in  $N$ -body galaxies within which a considerable amount of angular momentum was exchanged are quite different from the properties of bars grown in  $N$ -body galaxies with little such exchange (Athanassoula & Misiriotis 2002; Athanassoula 2003). This includes the morphological, the photometrical and the kinematical properties.  $N$ -body galaxies with considerable angular momentum internal redistribution have strong bars which often have ansae and which, viewed side-on (i.e. edge-on with the line of sight along the bar minor axis), have a characteristic peanut or 'X'-like shape. On the contrary,  $N$ -body galaxies within which little angular momentum has been exchanged have weaker bars with no ansae and whose side-on shape is boxy. These two types, which we will hereafter refer to as MH and as MD bars, are just the two extremes of a continuous sequence, and intermediate strength bars correspond to an exchange of an intermediate amount of angular momentum.

Strong differences between the MH and the MD types can be seen in the ellipticity profiles, the bar shape and the radial projected density profiles along and perpendicular to the bar. Fig. 4 of

<sup>1</sup>Laboratoire d'Astrophysique de Marseille (LAM), UMR6110, Observatoire Astronomique de Marseille Provence, CNRS/Université de Provence, Technopôle de Marseille-Etoile, 38 rue Frédéric Joliot Curie, 13388 Marseille Cédx 20, France (lia@oamp.fr, bosma@oamp.fr).

<sup>2</sup>Max-Planck-Institut für Astrophysik, Karl-Schwarzschild-Str. 1, D-85748 Garching bei München, Germany (dimitri@mpa-garching.mpg.de).

<sup>3</sup>Instituto Nacional de Astrofísica, Óptica, y Electrónica, Luis Enrique Erro 1, Tonantzintla, C.P. 72840, Puebla, México (carrasco@inaoep.mx, elsare@inaoep.mx).

<sup>4</sup>Departamento de Astronomía, Universidade de São Paulo, Rua do Matão 1226, 05508-090, São Paulo-SP, Brasil (ronaldo@astro.iag.usp.br).

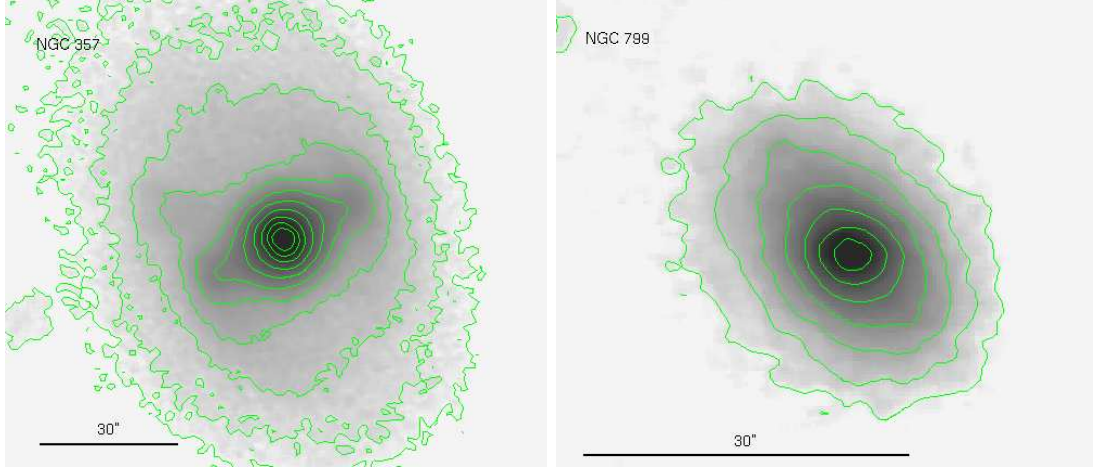


Fig. 1.  $J$  images of NGC 357 (left) and NGC 799 (right) with a few characteristic isophotes superposed.

Athanassoula & Misiriotis (2002) shows that in MH types there is an abrupt drop of the ellipticity at a location coinciding roughly with the end of the bar, while this feature is lacking from the radial ellipticity profiles of MD type  $N$ -body galaxies. Also the maximum ellipticity is much higher for MH types than for MDs.

MD type bars have isodensities which are well represented by ellipses. On the contrary MH types have a rather rectangular-like isodensities particularly in the outer parts of the bar. This can be quantified by the shape parameter  $c$ , which gives the shape of a generalised ellipse

$$(|x|/a)^c + (|y|/b)^c = 1. \quad (1)$$

Here  $a$  and  $b$  are the major and minor axes of the generalised ellipse and  $c$  is its shape parameter. Ellipses have  $c = 2$ , rectangular-like shapes have  $c > 2$  and lozenges  $c < 2$  (Athanassoula et al. 1990). Fitting the isodensities in the  $N$ -body images with generalised ellipses, Athanassoula & Misiriotis (2002) find that MH cases have considerably larger values of  $c$  than MD cases. Alternatively, it is possible to fit simple ellipses and measure their departure of the isodensities from the elliptical shape (Jedrzejewski 1987). This type of measurement also shows that the shape of the isodensities in MH type bars departs considerably from ellipses, contrary to MD types.

Finally, Athanassoula & Misiriotis (2002) made projected radial density profiles along the minor and the major axes of their  $N$ -body bars. They showed that the latter in MH types contributes a flat ledge, dropping abruptly at a radius which agrees with the end of the bar. On the other hand the radial pro-

jected density in the region of the bar in MD types shows only a gradual exponential-like decrease.

### 3. OBSERVATIONS

We observed a sample of nine barred galaxies in the  $J$  and  $K_s$  wavelengths using the CANICA near infrared (NIR) camera available at the 2.1-m telescope of the Observatorio Astrofísico Guillermo Haro (OAGH) in Cananea, Sonora, Mexico. Our aim is to compare real barred galaxies to  $N$ -body ones, and that has guided us in the choice of our sample. This consists of NGC 266, 357, 799, 1211, 1358, 1638, 7080, 7280 and 7743. Our images are deep and thus allowed us to trace the spiral arms for quite a large azimuthal angle and also to make sure that the outermost isophotes, which are used for the deprojection, are not much perturbed by the bar.

Here we will discuss more specifically two galaxies, NGC 357 and NGC 799, which we will compare to the  $N$ -body barred galaxies. Their  $J$  band images, on which we have superposed some characteristic isophotes, are given in Fig. 1. Images and results for the other galaxies in the sample can be found in Gadotti et al. (2007).

We used the IRAF task ELLIPSE to fit ellipses to the isophotes (Fig. 2), both as viewed on the sky and deprojected. For each isophote, this provides us with five very useful coefficients: the mean intensity along the ellipse and the  $a_2$ ,  $b_2$ ,  $a_4$  and  $b_4$  coefficients of the  $\sin m\theta$  and  $\cos m\theta$  components for  $m = 2$  and 4. In the outer parts, the  $m = 2$  components give us information on the position and inclination angle of the galaxy as projected on the sky and the  $m = 4$  components are very small. At radii where the bar is the dominant component, the  $m = 2$  components

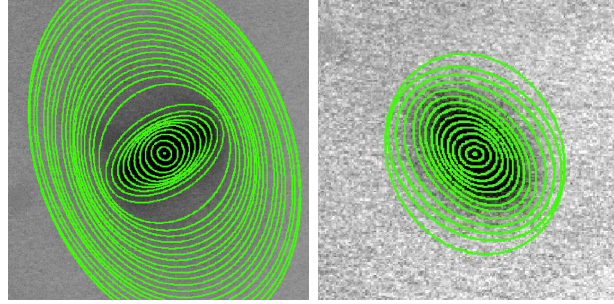


Fig. 2.  $J$  images of NGC 357 (left) and NGC 799 (right) with, superposed, a few of the fitted ellipses.

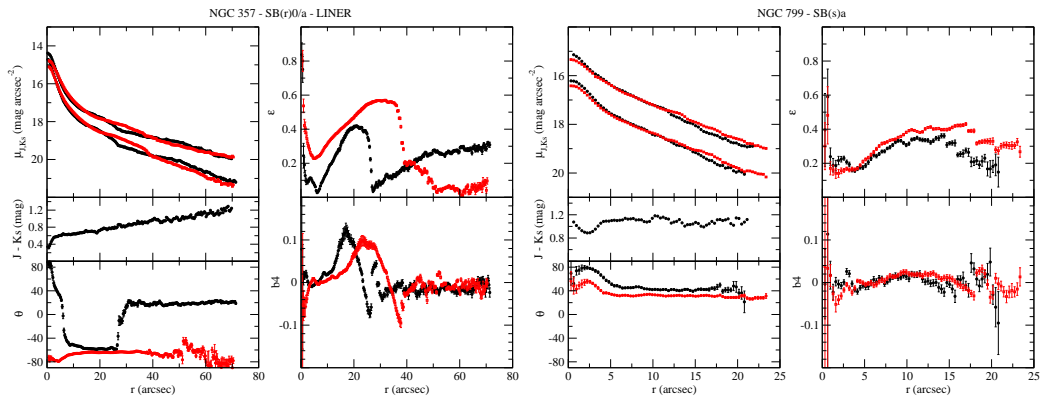


Fig. 3. Results of the ellipse fit for NGC 357 (left) and NGC 799 (right). These include the projected surface brightness in  $J$  and  $K_s$  (upper left), the  $J - K_s$  colour (center left), the ellipse position angle measured from north to east (bottom left), ellipticity (upper right) and the  $b_4$  Fourier coefficient (bottom right). These are given both for the direct and the deprojected views, the latter plotted in the online version in red.

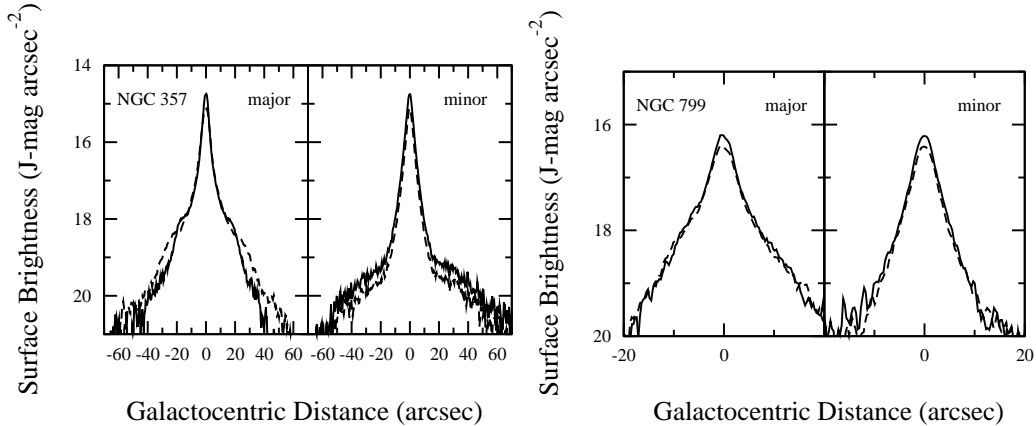


Fig. 4.  $J$  band projected surface brightness profiles along the bar major and minor axes. The results for the deprojected images are given with a dashed line.

provide the bar axial ratio and orientation and the  $m = 4$  the departure of its shape from a pure ellipse. All this information is given in Fig. 3.

We note that the radial profiles have quite different characteristics for the two galaxies. The biggest difference concerns the ellipticity radial profile. In NGC 357 this quantity rises gradually with distance from the center, reaches a maximum and then drops very steeply. On the other hand, in NGC 799 the gradual rise and maximum are followed by a very gradual decrease. This difference was also seen in the simulations, where MH type models show an abrupt drop which lacks from MD types (Athanassoula & Misiriotis 2002, and previous section). The maximum value of the ellipticity differs considerably between the two galaxies. For the deprojected images, it reaches about 0.6 for NGC 357, compared to 0.4 for NGC 799. Again, this difference is characteristic of MH and MD  $N$ -body galaxies (Athanassoula & Misiriotis 2002, and previous section).

Note also that the  $b_4$  coefficient is much larger for NGC 357 than for NGC 799, the two maxima being of the order of 0.1 and 0.01, respectively. This again is a characteristic difference between MH and MD types.

We also made radial surface brightness profiles along the bar major and minor axes and give the result in Fig. 4. For NGC 357 there are considerable differences between the profiles along these two directions. Along the major axis the bar contributes a flat section to the profile, followed by a very steep drop where it ends and joins the disc. This is absent on the minor axis radial profile. On the other hand NGC 799 shows no flat component corresponding to the bar and the profiles along the bar major and minor axes are very similar. Again, this behaviour is exactly what is expected from MH and MD  $N$ -body bars (Athanassoula & Misiriotis 2002, and previous section).

#### 4. CONCLUSIONS

We can thus come to the conclusion that  $N$ -body simulations reproduce well the properties of real bars and that NGC 357 is an MH type bar, while NGC 799 is an MD type. This means that a considerable amount of angular momentum was emitted by the near-resonant material in the bar region of NGC 357 and absorbed by near-resonant material in its outer disc and mainly its halo. On the other hand, much less angular momentum must have been exchanged in NGC 799.

#### Acknowledgments

It is a pleasure for EA and AB to thank the organisers for inviting them to this interesting meeting. We also thank ECOS and ANUIES for financing the exchange project M04U01, the Agence Nationale pour la Recherche for grant ANR-06-BLAN-0172 and FAPESP for grants 03/07099-0 and 00/06695-0. DAG, EA and AB would like to thank INAOE for their kind hospitality, both in the Tonanzintla and the Cananea sites. DAG thanks the CNRS for a 6 month poste rouge during which the data were analysed and the project started. DAG is supported by the Deutsche Forschungsgemeinschaft priority program 1177 (“Witnesses of Cosmic History: Formation and evolution of galaxies, black holes and their environment”), and the Max Planck Society. CANICA was developed under CONACYT project G28586E (PI: L. Carrasco). Figures 2, 3 and 4 are part of Figures 2 and 3 of Gadotti et al. (2007), which is published by Blackwell publishers in ‘Monthly Notices of the Royal Astronomical Society’ and is available at [www.blackwell-synergy.com](http://www.blackwell-synergy.com).

#### REFERENCES

- Athanassoula, E. 2002, ApJL, 569, 83
- Athanassoula, E. 2003, MNRAS, 341, 1179
- Athanassoula, E., Misiriotis, A. 2002, MNRAS, 330, 35
- Athanassoula E., Morin, S., Wozniak, H., Puy, D., Pierce, M., Lombard, J., Bosma, A., 1990, MNRAS, 245, 130
- de Vaucouleurs, G., de Vaucouleurs, A., Corwin, H. G., Jr., Buta, R. J., Paturel, G., Fouque, P. 1991, ‘Third Reference Catalogue of Bright Galaxies’, Springer-Verlag Berlin
- Eskridge, P. B. et al. 2000, AJ, 119, 536
- Gadotti, D., Athanassoula, E., Carrasco, L., Bosma, A., de Souza, R., Recillas, E. 2007, MNRAS, 381, 943
- Jedrzejewski, R. I. 1987, MNRAS, 226, 747
- Knapen, J. H., Shlosman, I., Peletier, R. F. 2000, ApJ, 529, 93
- Marinova, I., & Jogee, S. 2007, ApJ, 659, 1176
- Menendez-Delmestre, K., Sheth, K., Schinnerer, E., Jarrett, T. H., & Scoville, N. Z. 2007, ApJ, 657, 790